AGU PUBLICATIONS

JGR

Journal of Geophysical Research: Space Physics

RESEARCH ARTICLE
10.1002/2015JA022276

Special Section:
Energetic Electron Loss and its Impacts on the Atmosphere

Key Points:
- New numerical model for computation of ion production due to precipitating electrons
- Ionization yield functions for precipitating electrons tables
- An application of the model for computation of electron impact ionization is demonstrated

Supporting Information:
- Table S1

Correspondence to:
A. L. Mishev,
alex_mishev@yahoo.com

Citation:
Artamonov, A. A., A. L. Mishev, and I. G. Usoskin (2016), Model CRAC:EPII for atmospheric ionization due to precipitating electrons: Yield function and applications, *J. Geophys. Res. Space Physics*, *121*, 1736–1743, doi:10.1002/2015JA022276.

Received 16 DEC 2015
Accepted 27 JAN 2016
Accepted article online 29 JAN 2016
Published online 23 FEB 2016

Model CRAC:EPII for atmospheric ionization due to precipitating electrons: Yield function and applications

A. A. Artamonov[1], A. L. Mishev[2], and I. G. Usoskin[1,2]

[1] Sodankylä Geophysical Observatory (Oulu unit), University of Oulu, Oulu, Finland, [2] ReSoLVE Centre of Excellence, University of Oulu, Oulu, Finland

Abstract A new model of the family of CRAC models, CRAC:EPII (Cosmic Ray Atmospheric Cascade: Electron Precipitation Induced Ionization), is presented. The model calculates atmospheric ionization induced by precipitating electrons and uses the formalism of ionization yield functions. The CRAC:EPII model is based on a full Monte Carlo simulation of electron propagation and interaction with the air molecules. It explicitly considers various physical processes, namely, pair production, Compton scattering, generation of bremsstrahlung high-energy photons, photoionization, annihilation of positrons, and multiple scattering. The simulations were performed using GEANT 4 simulation tool PLANETOCOSMICS with NRLMSISE 00 atmospheric model. The CRAC:EPII model is applicable to the entire atmosphere. The results from the simulations are given as look-up table representing the ionization yield function. The table allows one to compute ionization due to precipitating electrons for a given altitude and location considering a given electron spectrum. Application of the model for computation of ion production during electron precipitation events using spectra from balloon-borne measurements is presented.

1. Introduction

Nowadays, an important topic in atmospheric and space physics is related to the potential influence of energetic particles, entering into the atmosphere, on various atmospheric processes. The induced atmospheric ionization can affect various atmospheric processes, global electric circuit, and minor constituents [e.g., *Vitt and Jackman*, 1996; *Turunen et al.*, 2009; *Krivolutsky et al.*, 2005; *Randall et al.*, 2007; *Damiani et al.*, 2008; *Jackman et al.*, 2008; *Vainio et al.*, 2009; *Calisto et al.*, 2011; *Jackman et al.*, 2011; *Mironova et al.*, 2012; *Rozanov et al.*, 2012; *Sinnhuber et al.*, 2012].

Different populations of ionizing particles are involved in the process of atmospheric ionization [*Bazilevskaya et al.*, 2008; *Mironova et al.*, 2015, and references therein]. Energetic particles are the main sources of ionization below 100 km, while solar UV and X-rays dominate at altitudes above 100 km but are absorbed below. Natural radionuclides (from the soil) contribute to atmospheric ionization in the lower atmosphere [*Eisenbud and Gesell*, 1997; *Balanov et al.*, 2008].

Energetic precipitating particles include galactic cosmic rays (GCRs), solar energetic particles (SEPs), precipitating protons, relativistic electrons from radiation belts, and auroral electrons. In this work we focus on relativistic electrons, while other sources are considered elsewhere.

The main source of ionization in the troposphere and stratosphere is related to GCR, which induce a complicated nuclear-electromagnetic-muon cascade [*O'Brien et al.*, 1997; *Usoskin and Kovaltsov*, 2006; *Bazilevskaya et al.*, 2008; *Stozhkov et al.*, 2009; *Usoskin et al.*, 2009; *Velinov et al.*, 2013]. GCRs originate from outer space and are mostly protons and α particles [e.g., *Gaisser and Stanev*, 2010]. The intensity of GCR is modulated by the solar wind and follows the inverse 11 year solar cycle. An important sporadic source of ionization is related to SEPs, linked to eruptive solar processes such as solar flares and coronal mass ejections [see *Reames*, 1999; *Cliver et al.*, 2004; *Dorman*, 2006; *Reames*, 2009a, 2009b; *Aschwanden*, 2012, and references therein]. In some cases the energy of SEPs is high enough (about a 1 GeV/nucleon) to initiate an atmospheric cascade leading to an enhancement of count rate of ground-based neutron monitors. This special class of SEP events, called ground level enhancements, significantly increases the ion production in the atmosphere, specifically in polar regions [*Damiani et al.*, 2008; *Jackman et al.*, 2009; *Calisto et al.*, 2011; *Jackman et al.*, 2011; *Usoskin et al.*, 2011; *Mironova et al.*, 2012; *Mishev et al.*, 2013; *Mishev and Velinov*, 2015].

The precipitating electrons ionize the atmosphere, specifically its upper polar part. Electrons precipitate into the atmosphere from different regions of the magnetosphere due to various mechanisms such as nonlinear wave-particle interactions [e.g., *Rees*, 1963; *Dorman*, 2004; *Millan and Thorne*, 2007; *Horne et al.*, 2009; *Meredith et al.*, 2011; *Carson et al.*, 2013; *Tsurutani et al.*, 2013; *Usanova et al.*, 2014; *Kubota et al.*, 2015; *Mironova et al.*, 2015; *Miyoshi et al.*, 2015, and references therein]. Precipitating electrons play an important role in ion production in the Earth's atmosphere, specifically in the upper atmosphere over polar regions [*Makhmutov et al.*, 2003; *Clilverd et al.*, 2008; *Daae et al.*, 2012; *Clilverd et al.*, 2013]. Precipitating electrons affect the atmospheric chemistry [e.g., *Callis*, 1991; *Callis et al.*, 1996; *Rozanov et al.*, 2005; *Verronen et al.*, 2011; *Daae et al.*, 2012; *Andersson et al.*, 2014; *Mironova et al.*, 2015] as well as several physical properties of the atmosphere and magnetosphere [e.g., *Makhmutov et al.*, 2003; *Clilverd et al.*, 2008; *Maliniemi et al.*, 2013]. The intensity of the electron precipitation depends on solar and geomagnetic activity [*Onsager et al.*, 2002; *Reeves et al.*, 2003; *Makhmutov et al.*, 2006; *Rodger et al.*, 2007; *Horne et al.*, 2009; *Park et al.*, 2013; *Neal et al.*, 2015].

In this work we focus on precipitation of electrons and present a model based on full Monte Carlo simulation of their propagation in the Earth's atmosphere. The model allows one to assess the atmospheric ionization due to precipitating electrons.

2. The Model CRAC:EPII

Ion production in the atmosphere induced by precipitating electrons can be assessed by parametrization-driven models [e.g., *Fang et al.*, 2008, 2010; *McGranaghan et al.*, 2015]. On the other hand, Monte Carlo models realistically simulate electron transport in the atmosphere considering explicitly their interaction with matter [*Berger and Seltzer*, 1972; *Berger et al.*, 1974; *Sternheimer et al.*, 1984; *Solomon*, 1993; *Wissing and Kallenrode*, 2009]. The main advantage of Monte Carlo transport codes is that they consider realistically all the physics processes involved, namely, energy deposition, pair production, Compton scattering, generation of bremsstrahlung high-energy photons (henceforth bremsstrahlung), photoionization, and annihilation of positrons [*Berger and Seltzer*, 1972; *Berger et al.*, 1974; *Wissing and Kallenrode*, 2009]. In addition, they allow one to consider deeper penetrating bremsstrahlung compared to primary charged particles [e.g., *Berger and Seltzer*, 1972; *Schröter et al.*, 2006], which contribute to ionization of air, specifically at lower and middle altitudes. Therefore, in this work we apply a Monte Carlo simulation of electron propagation and interaction with atmospheric molecules.

An example of Monte Carlo models is the Atmospheric Ionization Model Osnabrück (AIMOS); for details see *Wissing and Kallenrode* [2009]. It is a Monte Carlo simulation model including a sorting algorithm to use observations from satellites. The model provides 3-D ion pair production rates for precipitating solar and magnetospheric charged particles and demonstrates good agreement with earlier models. It implies that the major contribution to ionospheric ionization is due to solar electrons in polar caps as well as magnetospheric electrons in the auroral oval. However, this model requires a complicated interface and it is computationally time consuming.

In this study, propagation and interaction of precipitating electrons with the atmospheric molecules are simulated with the (Geometry and Tracking) GEANT4-based [*Agostinelli et al.*, 2003] simulation tool PLANETOCOSMICS [*Desorgher et al.*, 2005] code with the NRLMSISE 00 atmospheric model employed [*Picone et al.*, 2002]. The PLANETOCOSMICS is a tool for detailed simulation of particle interaction with atmospheric molecules and atoms. The code simulates the interactions and, when appropriate, decays of nuclei, hadrons, muons, electrons, and photons in the atmosphere in a wide energy range. It yields detailed information about the secondary particle flux at a selected observation level and the energy deposition.

Using PLANETOCOSMICS we have computed the ionization yield function, i.e., the number of ion pairs produced in the ambient air at a given atmospheric depth by a single primary vertically precipitating electron with a given energy. The ionization yield function $Y_e(x, K)$ (ion pairs $\cdot$ cm^2/g) at a given atmospheric depth x is defined as

$$Y_e(x, K) = \frac{\partial E}{E_{\text{ion}} \partial x} \tag{1}$$

where ∂E is the mean energy loss in the atmospheric layer ∂x at depth x per one simulated primary electron with kinetic energy K and $E_{\text{ion}} = 35$ eV is the average energy necessary for production of an ion pair in air [*Porter et al.*, 1976].

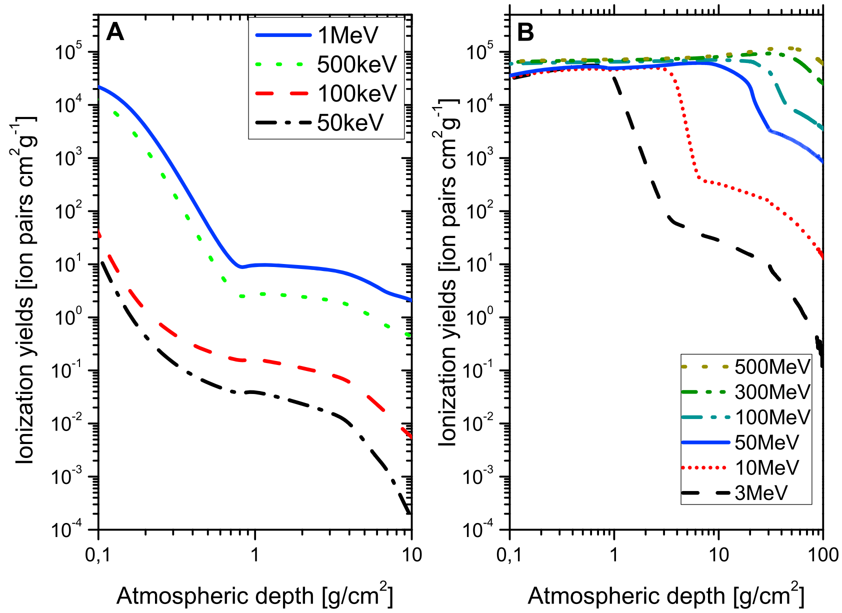

Figure 1. $Y_e(x, K)$ for precipitating electrons with different energies as a function of atmospheric depth computed with the CRAC:EPII model. (a) $Y_e(x, K)$ for precipitating electrons with energies from 50 keV to 1 MeV as denoted in the legend. (b) $Y_e(x, K)$ for precipitating electrons with energies from 3 MeV to 500 MeV as denoted in the legend. The curves are smooth fits of the computed data points. The corresponding look-up table is given in Appendix A.

The computations were carried out in the energy range of precipitating electrons between 20 keV and 500 MeV. An example of $Y_e(x, K)$ for several energies of the primary electron is given in Figure 1. The corresponding look-up table is given in Appendix A. One can see the essential contribution of bremsstrahlung, specifically at depths below 1 g/cm^2 for lower energies (20 keV to 1 MeV, Figure 1a), below 10 g/cm^2 for precipitating electrons with energy of 10 MeV, and below 30 g/cm^2 for precipitating electrons with energy greater than 10 MeV (Figure 1b).

The ionization yield function $Y_e(x, K)$ is related to ion production rate $Q(x)$ at a given depth x as

$$Q(x) = \int_{E_i}^{\infty} \frac{\mathrm{d}J_e(K)}{\mathrm{d}K} Y_e(x, K)\mathrm{d}K \quad (2)$$

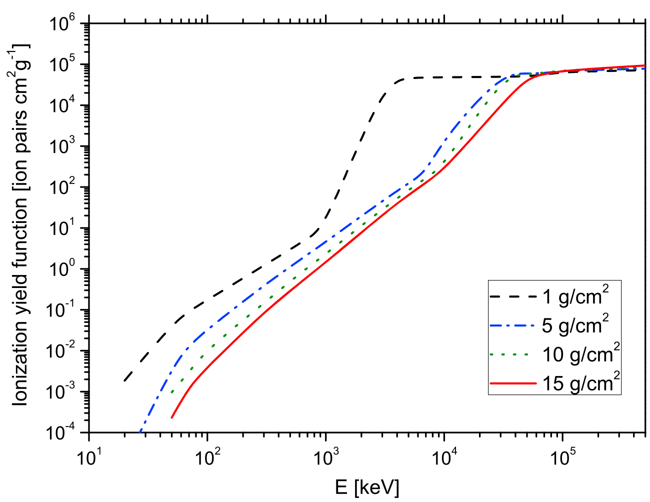

Figure 2. Ionization yield function for precipitating electrons at several depths, namely, 1, 5, 10, and 15 g/cm^2. Different curves correspond to different atmospheric depths as denoted in the legend. The curves are smooth fits of the computed data points. The corresponding look-up table is given in Appendix A.

where $\frac{\mathrm{d}J_e(K)}{\mathrm{d}K}$ is the differential energy spectrum of the primary precipitating electrons with energy K. The integration is over the kinetic energy above E_i, which is 20 keV in our model. Here the yield function $Y_e(x, K)$ is the response (in the sense of ionization yields) to the monoenergetic unit flux of the primary precipitating electron entering the Earth's atmosphere with a vertical incidence. Therefore, the CRAC:EPII model follows the formalism described in *Usoskin and Kovaltsov* [2006]. The model makes it possible to compute ion production due to precipitating electrons in the whole atmosphere in any location over the globe considering given spectrum of electrons $J_e(K)$. An example of ionization yield function for precipitating

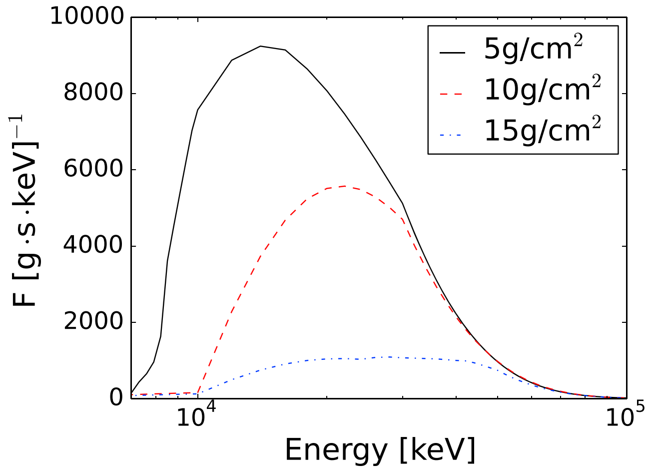

Figure 3. Differential ionization function F for precipitating electrons at several depths. Different curves correspond to different atmospheric depths as denoted in the legend. The precipitating electrons spectrum corresponds to spectrum 4 in Table 1 and Figure 4.

electrons at several depths, namely, 1, 5, 10, and 15 g/cm^2 is shown in Figure 2. The shape of the ionization yield function is similar at depths lower than 5 g/cm^2, but it is different at smaller depths of a 1 g/cm^2, where a spike is observed.

The model was quantitatively compared with a recent parametrization-driven model [*Fang et al.*, 2008, 2010] assuming a monoenergetic ionization yields with a very good agreement achieved (see A. Artamonov et al., Atmospheric ionization induced by precipitating electrons: Comparison of CRAC:EPII model with a parametrization model, submitted manuscript, 2016, http://arxiv.org/pdf/1601.0591-0v1.pdf). In general, the CRAC:EPII model yields slightly more ions, specifically in the maximum compared to the parametrization of *Fang et al.* [2010]. In addition, the level of maximum ion production by CRAC:EPII is at slightly smaller altitudes compared to the parametrization, because of the contribution of bremsstrahlung, which is neglected in the parametrization.

3. Application of the Model

With the described above formalism it is possible to compute the ion production in the atmosphere due to precipitating electrons (equation (2)). The differential ionization function F, defined as a product of the ionization yield function (Figure 2) and a given spectrum of precipitating electrons (see below), is shown in Figure 3 for several depths. For the computation we assumed a hard precipitating electron spectrum (spectrum 4 from Table 1; see also Figure 4). One can see that the most effective energy of precipitating electrons to induce ionization strongly depends on the atmospheric depth. The bulk of ionization at depth of about 5 g/cm^2 is due to electrons with energy of about 10 MeV, while at depth of about 10 g/cm^2 is mostly produced by particles with energy of about 200 MeV. Therefore, the maximum shifts to higher energies with decreasing the altitude (increasing the depth). At depths of about 15 g/cm^2 the differential ionization function F flattens, because of the diminishing number of high-energy precipitating electrons.

In order to compute the ion production in the atmosphere due to precipitating electrons, a precise information about their spectra is necessary, which is usually derived on the basis of various measurements and reconstructions. Here we use electron spectra derived on the basis of balloon-borne measurements, specifically performed at polar latitudes [*Bazilevskaya and Makhmutov*, 1999]. The spectra are available in a recently published catalogue, summarizing 58 years measurements, namely, electron precipitation events observed in the polar atmosphere during the period 1961–2014 in the framework of cosmic ray observations performed in the stratosphere by Lebedev Physical Institute of Russian Academy of Sciences [*Makhmutov et al.*, 2015].

Table 1. Four Electron Precipitation Events Selected in This Study[a]

N	Date	A_e (cm^2 s keV)$^{-1}$	E_0 (keV)
1	16 August 2002	1.37×10^4	1.40×10^1
2	7 October 2002	7.77×10^2	1.17×10^2
3	19 September 2003	3.40×10^0	1.99×10^3
4	27 March 2013	1.11×10^0	1.18×10^4

[a]They were recorded during long-term balloon-borne cosmic ray measurements in the stratosphere at the polar station of Murmansk region (67°33′N, 33°20′E) [*Makhmutov et al.*, 2015]. A_e is the scaling parameter of the flux of the incident electrons; accordingly, E_0 is the characteristic energy of the electron spectra (see equation (3)).

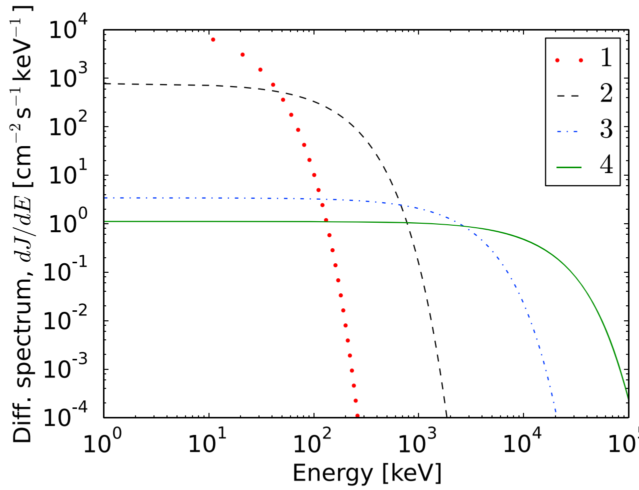

Figure 4. Differential spectra of precipitating electrons considered in this study according to equation (3). The parameters of the spectra are given in Table 1. The number of the spectrum in the legend corresponds to those in Table 1.

In the study presented here we assume an exponential shape of the precipitating electrons spectrum similarly to [e.g., *Millan et al.*, 2007; *Comess et al.*, 2013]

$$\frac{dJ_e(K)}{dK} = A_e \cdot \exp(-K/E_0) \quad (3)$$

where E_0 is a characteristic energy in the range of a keV to a MeV, A_e is a scale of the flux of incident electrons given in $[\mathrm{cm}^2\ \mathrm{s\ keV}]^{-1}$, and K is the electron's kinetic energy. The used spectra are summarized in Table 1 and shown in Figure 4. They cover several orders of magnitude and encompass most of the performed measurements over the years, namely, between a soft spectrum 1 (16 August 2002) and a very hard spectrum 4 (27 March 2013). Detailed study of the electron impact ionization in the atmosphere considering the published catalogue is beyond the topic of this work. The computed ion production rates in the atmosphere for the events from Table 1 are shown in Figure 5.

The contribution of bremsstrahlung to ion production is clearly seen at depths below 0.4 g/cm^2 for spectrum 2, accordingly below 5 g/cm^2 for spectrum 3, and below 10 g/cm^2 for spectrum 4. The contribution of bremsstrahlung to ion production due to precipitating electrons varies as a function of the precipitating electron spectrum. The harder spectra result on a deeper depth of bremsstrahlung contribution to ion production.

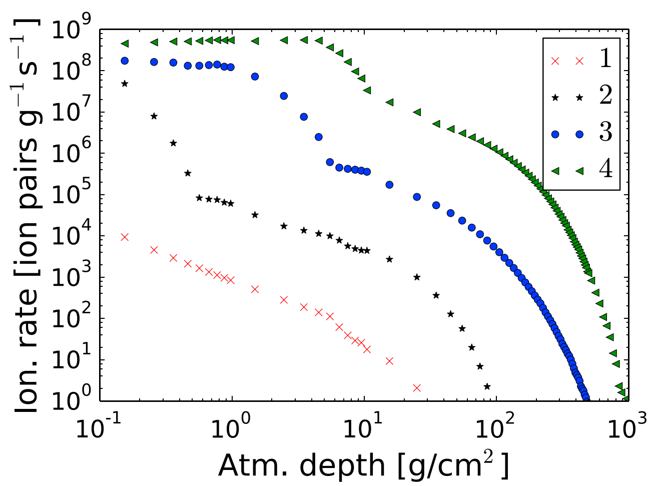

Figure 5. Ion production rate in the atmosphere as a function of the atmospheric depth due to precipitating electrons for spectra given in Table 1 and Figure 4. The number of the spectrum in the legend corresponds to those in Table 1.

4. Conclusion

Here we have presented a full numerical model aiming computation of ion production in the Earth's atmosphere due to precipitating electrons. It is based on a realistic simulation of propagation and interaction of precipitating electrons with the air using the PLANETOCOSMICS code [*Picone et al.*, 2002; *Desorgher et al.*, 2005]. The model allows computations in the whole atmosphere, specifically in the stratosphere over the globe, since it is based on the yield function formalism. The model is an extension of cosmic ray ionization model CRAC. The ionization yield functions for precipitating electrons with vertical incidence are given in a look-up Table A1; accordingly, an electronic table with more detailed computations is available upon request.

Using the model, one can compute the precipitating electrons induced ionization in the atmosphere for any desired location and conditions considering a given precipitating electrons spectrum. The model allows evaluation of the electron impact ionization in the atmosphere under different conditions and will stimulate better understanding on various atmospheric processes [e.g., *Mironova et al.*, 2015, and references therein]. An application of the model for computation of electron impact ionization in the atmosphere using spectra derived on the basis of balloon-borne measurements is demonstrated in section 3.

Appendix A: Ionization Yields for Precipitating Electrons: A Look-Up Table

Here in Table A1, we present ionization yield function for precipitating electrons in the form of a look-up table. The ionization yield functions (equation (1)) are computed with the GEANT4-based [*Agostinelli et al.*, 2003] PLANETOCOSMICS [*Desorgher et al.*, 2005] code using NRLMSISE 00 atmospheric model [*Picone et al.*, 2002]. The lines represent the ionization yield function at the given depth in the atmosphere. The first column is the atmospheric depth.

Table A1. Ionization Yield Function (Ion Pairs cm^2/g) for Precipitating Electrons With Vertical Incidence With Various Energy as a Function of the Atmospheric Depth Computed With CRAC:EPII Model[a]

Depth (g/cm^2)	20 (keV)	70 (keV)	100 (keV)	500 (keV)	1 (MeV)	5 (MeV)	10 (MeV)	50 (MeV)	100 (MeV)	500 (MeV)
0.15	8.53×10^{-2}	5.18×10^{-1}	8.99×10^{-1}	1.23×10^{4}	3.19×10^{4}	3.57×10^{4}	3.59×10^{4}	4.09×10^{4}	6.06×10^{4}	6.87×10^{4}
0.46	9.63×10^{-3}	2.08×10^{-1}	3.76×10^{-1}	5.13×10^{0}	2.83×10^{3}	3.10×10^{4}	2.94×10^{4}	3.39×10^{4}	6.38×10^{4}	7.07×10^{4}
1	4.63×10^{-4}	4.87×10^{-2}	1.03×10^{-1}	2.09×10^{0}	7.09×10^{0}	5.70×10^{4}	5.30×10^{4}	5.38×10^{4}	6.61×10^{4}	7.29×10^{4}
3	6.52×10^{-5}	2.00×10^{-2}	4.57×10^{-2}	1.28×10^{0}	4.81×10^{0}	1.34×10^{2}	5.03×10^{4}	5.87×10^{4}	6.82×10^{4}	7.56×10^{4}
5	3.60×10^{-5}	1.53×10^{-2}	3.57×10^{-2}	1.10×10^{0}	4.23×10^{0}	1.22×10^{2}	2.05×10^{4}	6.01×10^{4}	6.89×10^{4}	7.69×10^{4}
10	0	2.59×10^{-3}	7.27×10^{-3}	4.41×10^{-1}	2.32×10^{0}	8.44×10^{1}	3.25×10^{2}	5.90×10^{4}	7.10×10^{4}	8.55×10^{4}
15	0	1.90×10^{-3}	9.27×10^{-3}	7.04×10^{-1}	3.28×10^{0}	9.74×10^{1}	3.50×10^{2}	4.89×10^{4}	7.06×10^{4}	9.32×10^{4}
25	0	2.59×10^{-4}	1.01×10^{-3}	1.11×10^{-1}	6.36×10^{-1}	3.91×10^{1}	1.77×10^{2}	6.59×10^{3}	5.61×10^{4}	1.07×10^{5}
35	0	4.54×10^{-5}	2.16×10^{-4}	4.31×10^{-2}	2.74×10^{-1}	2.37×10^{1}	1.21×10^{2}	2.99×10^{3}	2.75×10^{4}	1.16×10^{5}
55	0	9.54×10^{-6}	6.98×10^{-5}	6.42×10^{-3}	5.14×10^{-2}	9.23×10^{0}	5.86×10^{1}	1.99×10^{3}	7.57×10^{3}	1.13×10^{5}
105	0	0	0	6.80×10^{-5}	7.70×10^{-4}	1.12×10^{0}	1.19×10^{1}	7.71×10^{2}	3.28×10^{3}	5.53×10^{4}
155	0	0	0	0	2.98×10^{-5}	1.82×10^{-1}	2.85×10^{0}	3.16×10^{2}	1.47×10^{3}	2.78×10^{4}
205	0	0	0	0	0	3.94×10^{-2}	8.13×10^{-1}	1.33×10^{2}	6.67×10^{2}	1.45×10^{4}
255	0	0	0	0	0	6.75×10^{-3}	2.35×10^{-1}	5.72×10^{1}	3.01×10^{2}	7.33×10^{3}
305	0	0	0	0	0	1.18×10^{-3}	6.44×10^{-2}	2.47×10^{1}	1.41×10^{2}	3.68×10^{3}
355	0	0	0	0	0	2.76×10^{-5}	2.73×10^{-2}	1.05×10^{1}	6.32×10^{1}	1.80×10^{3}
455	0	0	0	0	0	0	1.35×10^{-3}	2.02×10^{0}	1.30×10^{1}	4.34×10^{2}
560	0	0	0	0	0	0	2.34×10^{-5}	3.82×10^{-1}	2.78×10^{0}	9.35×10^{1}
760	0	0	0	0	0	0	0	1.03×10^{-2}	1.50×10^{-1}	4.95×10^{0}
880	0	0	0	0	0	0	0	5.78×10^{-4}	1.93×10^{-2}	6.86×10^{-1}
920	0	0	0	0	0	0	0	1.09×10^{-4}	4.68×10^{-2}	3.94×10^{-1}
1000	0	0	0	0	0	0	0	0	0	4.50×10^{-2}

[a]The propagation of precipitating electrons in the atmosphere is performed with the PLANETOCOSMICS code using NRLMSISE 00 atmospheric model [*Picone et al.*, 2002; *Desorgher et al.*, 2005].

Acknowledgments
We warmly acknowledge colleagues from ISSI project "Specification of ionization sources affecting atmospheric processes" led by Irina Mironova, specifically J. Wissing for the discussions related to AIMOS model and V. Makhmutov and G. Bazilevskaya for their fruitful discussions about electron precipitation events and their spectra. This work was supported by the Center of Excellence ReSoLVE (project 272157) of the Academy of Finland. A. Artamonov is supported by Thule institute, Oulu University (project 24002201). Any additional data may be obtained from Oulu cosmic ray station (e-mail: ilya.usoskin@oulu.fi) and https://cosmicrays.oulu.fi/. The authors would like to thank the anonymous reviewers for their insightful comments and suggestions that have contributed to improve this paper.

References

Agostinelli, S., J. Allison, and K. Amako (2003), GEANT 4 — A simulation toolkit, *Nucl. Instrum. Methods Phys. Res., Sect. A*, *506*(3), 250–303.

Andersson, M., P. Verronen, C. Rodger, M. Clilverd, and A. Seppälä (2014), Missing driver in the Sun-Earth connection from energetic electron precipitation impacts mesospheric ozone, *Nat. Commun.*, *5*, 5197.

Aschwanden, M. (2012), GeV particle acceleration in solar flares and ground level enhancement (GLE) events, *Space Sci. Rev.*, *171*(1–4), 3–21.

Balanov, M., et al. (2008), *Sources and Effects of Ionizing Radiation. UNSCEAR 2008 Report to the General Assembly With Scientific Annexes*, Volume II scientific Annexe B Exposures of the Public and Workers from Various Sources of Radiation, New York, U. N.

Bazilevskaya, G., and V. Makhmutov (1999), Precipitations of energetic electrons into atmosphere according to the data using Zond particle measurements, *Izv. Akad. Nauk. Ser. Fizicheskaya*, *63*(8), 1670–1674.

Bazilevskaya, G. A., et al. (2008), Cosmic ray induced ion production in the atmosphere, *Space Sci. Rev.*, *137*, 149–173.

Berger, M., and S. Seltzer (1972), Bremsstrahlung in the atmosphere, *J. Atmos. Terr. Phys.*, *34*(1), 85–108.

Berger, M., S. Seltzer, and K. Maeda (1974), Some new results on electron transport in the atmosphere, *J. Atmos. Terr. Phys.*, *36*(4), 591–617.

Calisto, M., I. Usoskin, E. Rozanov, and T. Peter (2011), Influence of Galactic Cosmic Rays on atmospheric composition and dynamics, *Atmos. Chem. Phys.*, *11*(9), 4547–4556.

Callis, L. (1991), Precipitating relativistic electrons: Their long-term effect on stratospheric odd nitrogen levels, *J. Geophys. Res.*, *96*(D2), 2939–2976.

Callis, L., R. Boughner, D. Baker, R. Mewaldt, J. Bernard Blake, R. Selesnick, J. Cummings, M. Natarajan, G. Mason, and J. Mazur (1996), Precipitating electrons: Evidence for effects on mesospheric odd nitrogen, *Geophys. Res. Lett.*, *23*(15), 1901–1904.

Carson, B., C. Rodger, and M. Clilverd (2013), POES satellite observations of EMIC-wave driven relativistic electron precipitation during 1998–2010, *J. Geophys. Res. Space Physics*, *118*, 232–243, doi:10.1029/2012JA017998.

Clilverd, M., et al. (2008), Energetic electron precipitation during substorm injection events: High-latitude fluxes and an unexpected midlatitude signature, *J. Geophys. Res.*, *113*, A10311, doi:10.1029/2008JA013220.

Clilverd, M., N. Cobbett, C. Rodger, J. Brundell, M. Denton, D. Hartley, J. Rodriguez, D. Danskin, T. Raita, and E. Spanswick (2013), Energetic electron precipitation characteristics observed from Antarctica during a flux dropout event, *J. Geophys. Res. Space Physics*, *118*(11), 6921–6935, doi:10.1002/2013JA019067.

Cliver, E., S. Kahler, and D. Reames (2004), Coronal shocks and solar energetic proton events, *Astrophys. J.*, *605*, 902–910.

Comess, M., D. Smith, R. Selesnick, R. Millan, and J. Sample (2013), Duskside relativistic electron precipitation as measured by SAMPEX: A statistical survey, *J. Geophys. Res. Space Physics*, *118*, 5050–5058, doi:10.1002/jgra.50481.

Daae, M., P. Espy, H. Nesse Tyssy, D. Newnham, J. Stadsnes, and F. Sraas (2012), The effect of energetic electron precipitation on middle mesospheric night-time ozone during and after a moderate geomagnetic storm, *Geophys. Res. Lett.*, *39*, L21811, doi:10.1029/2012GL053787.

Damiani, A., M. Storini, M. Laurenza, and C. Rafanelli (2008), Solar particle effects on minor components of the polar atmosphere, *Ann. Geophys.*, *26*(2), 361–370.

Desorgher, L., E. Flückiger, M. Gurtner, M. Moser, and R. Bütikofer (2005), A GEANT 4 code for computing the interaction of cosmic rays with the Earth's atmosphere, *Int. J. Modern Phys. A*, *20*(A11), 6802–6804.

Dorman, L. (2004), *Cosmic Rays in the Earth's Atmosphere and Underground*, Kluwer Acad., Dordrecht, Netherlands.

Dorman, L. (2006), *Cosmic Ray Interactions, Propagation, and Acceleration in Space Plasmas, Astrophysics and Space Science Library 339*, Springer, Dordrecht, Netherlands.

Eisenbud, M., and T. Gesell (1997), *Environmental Radioactivity From Natural, Industrial and Military Sources*, Academic Press, San Diego, Calif.

Fang, X., C. Randall, D. Lummerzheim, S. Solomon, M. Mills, D. Marsh, C. Jackman, W. Wang, and G. Lu (2008), Electron impact ionization: A new parameterization for 100 eV to 1 MeV electrons, *J. Geophys. Res.*, *113*, A09311, doi:10.1029/2008JA013384.

Fang, X., C. Randall, D. Lummerzheim, W. Wang, G. Lu, S. Solomon, and R. Frahm (2010), Parameterization of monoenergetic electron impact ionization, *Geophys. Res. Lett.*, *37*, L22106, doi:10.1029/2010GL045406.

Gaisser, T. K., and T. Stanev (2010), Cosmic rays, in *Review of Particle Physics Particle Data Group, J. Phys. G: Nucl. Part Phys. 37*, edited by K. Nakamura et al., pp. 269–275, IOPscience, Bristol, U. K.

Horne, R., M. Lam, and J. Green (2009), Energetic electron precipitation from the outer radiation belt during geomagnetic storms, *Geophys. Res. Lett.*, *36*, L19104, doi:10.1029/2009GL040236.

Jackman, C., et al. (2008), Short- and medium-term atmospheric constituent effects of very large solar proton events, *Atmos. Chem. Phys.*, *8*(3), 765–785.

Jackman, C., D. Marsh, F. Vitt, R. Garcia, C. Randall, E. Fleming, and S. Frith (2009), Long-term middle atmospheric influence of very large solar proton events, *J. Geophys. Res. Atmos.*, *114*, D11304, doi:10.1029/2008JD011415.

Jackman, C., et al. (2011), Northern Hemisphere atmospheric influence of the solar proton events and ground level enhancement in January 2005, *Atmos. Chem. Phys.*, *11*(13), 6153–6166.

Krivolutsky, A., A. Kuminov, and T. Vyushkova (2005), Ionization of the atmosphere caused by solar protons and its influence on ozonosphere of the Earth during 1994–2003, *J. Atmos. Sol. Terr. Phys.*, *67*(1-2), 105–117.

Kubota, Y., Y. Omura, and D. Summers (2015), Relativistic electron precipitation induced by EMIC-triggered emissions in a dipole magnetosphere, *J. Geophys. Res. Space Physics*, *120*, 4384–4395, doi:10.1002/2015JA021017.

Makhmutov, V., G. Bazilevskaya, and M. Krainev (2003), Characteristics of energetic electron precipitation into the Earth's polar atmosphere and geomagnetic conditions, *Adv. Space Res.*, *31*(4), 1087–1092.

Makhmutov, V., G. Bazilevskaya, L. Desorgher, and E. Flückiger (2006), Observation of energetic electron precipitation into atmosphere in October 2003, *Bull. Russ. Acad. Sci.*, *69*(6), 990–993.

Makhmutov, V., G. Bazilevskaya, Y. Stozhkov, A. Svirzhevskaya, and N. Svirzhevsky (2015), Catalogue of electron precipitation events as observed in the long-duration cosmic ray balloon experiment, *J. Atmos. Sol. Terr. Phys.*, doi:10.1016/j.jastp.2015.12.006.

Maliniemi, V., T. Asikainen, K. Mursula, and A. Seppälä (2013), QBO-dependent relation between electron precipitation and wintertime surface temperature, *J. Geophys. Res. Atmos.*, *118*, 6302–6310, doi:10.1002/jgrd.50518.

McGranaghan, R., D. Knipp, S. Solomon, and X. Fang (2015), A fast, parameterized model of upper atmospheric ionization rates, chemistry, and conductivity, *J. Geophys. Res. Space Physics*, *120*, 4936–4949, doi:10.1002/2015JA021146.

Meredith, N., R. Horne, M. Lam, M. Denton, J. Borovsky, and J. Green (2011), Energetic electron precipitation during high-speed solar wind stream driven storms, *J. Geophys. Res.*, *116*, A05223, doi:10.1029/2010JA016293.

Millan, R., and R. Thorne (2007), Review of radiation belt relativistic electron losses, *J. Atmos. Sol. Terr. Phys.*, *69*(3), 362–377.

Millan, R., R. Lin, D. Smith, and M. McCarthy (2007), Observation of relativistic electron precipitation during a rapid decrease of trapped relativistic electron flux, *Geophys. Res. Lett.*, *34*, L10101, doi:10.1029/2006GL028653.

Mironova, I., I. Usoskin, G. Kovaltsov, and S. Petelina (2012), Possible effect of extreme solar energetic particle event of 20 January 2005 on polar stratospheric aerosols: Direct observational evidence, *Atmos. Chem. Phys.*, *12*(2), 769–778.

Mironova, I., K. Aplin, F. Arnold, G. Bazilevskaya, R. Harrison, A. Krivolutsky, K. Nicoll, E. Rozanov, E. Turunen, and I. Usoskin (2015), Energetic particle influence on the Earth's atmosphere, *Space Sci. Rev.*, *194*(1–4), 1–96.

Mishev, A., and P. Velinov (2015), Time evolution of ionization effect due to cosmic rays in terrestrial atmosphere during GLE 70, *J. Atmos. Sol. Terr. Phys.*, *129*, 78–86.

Mishev, A., P. Velinov, L. Mateev, and Y. Tassev (2013), Ionization effect of nuclei with solar and galactic origin in the Earth atmosphere during GLE 69 on 20 January 2005, *J. Atmos. Sol. Terr. Phys.*, *89*(1), 1–7.

Miyoshi, Y., et al. (2015), Energetic electron precipitation associated with pulsating aurora: EISCAT and Van Allen Probe observations, *J. Geophys. Res. Space Physics*, *120*(4), 2754–2766.

Neal, J., C. Rodger, M. Clilverd, N. Thomson, T. Raita, and T. Ulich (2015), Long-term determination of energetic electron precipitation into the atmosphere from AARDDVARK subionospheric VLF observations, *J. Geophys. Res. Space Physics*, *120*, 2194–2211, doi:10.1002/2014JA020689.

O'Brien, K., W. Friedberg, H. Sauer, and D. Smart (1997), Atmospheric cosmic rays and solar energetic particles at aircraft altitudes, *Environ. Int.*, *22*(SUPPL. 1), S9–S44.

Onsager, T., G. Rostoker, H.-J. Kim, G. Reeves, T. Obara, H. Singer, and C. Smithtro (2002), Radiation belt electron flux dropouts: Local time, radial, and particle-energy dependence, *J. Geophys. Res.*, *107*(A11), 1382, doi:10.1029/2001JA000187.

Park, M.-Y., D.-Y. Lee, D.-K. Shin, J.-H. Cho, and E.-H. Lee (2013), Dependence of energetic electron precipitation on the geomagnetic index Kp and electron energy, *J. Astron. Space Sci.*, *30*(4), 247–253.

Picone, J., A. Hedin, D. Drob, and A. Aikin (2002), NRLMSISE-00 empirical model of the atmosphere: Statistical comparisons and scientific issues, *J. Geophys. Res.*, *107*(A12), 1468, doi:10.1029/2002JA009430.

Porter, H., C. Jackman, and A. Green (1976), Efficiencies for production of atomic nitrogen and oxygen by relativistic proton impact in air, *J. Chem. Phys.*, *65*(1), 154–167.

Randall, C., V. Harvey, C. Singleton, S. Bailey, P. Bernath, M. Codrescu, H. Nakajima, and J. Russell (2007), Energetic particle precipitation effects on the Southern Hemisphere stratosphere in 1992–2005, *J. Geophys. Res.*, *112*, D08308, doi:10.1029/2006JD007696.

Reames, D. (1999), Particle acceleration at the Sun and in the heliosphere, *Space Sci. Rev.*, *90*(3–4), 413–491.

Reames, D. (2009a), Solar release times of energetic particles in ground-level events, *Astrophys. J.*, *693*(1), 812–821.

Reames, D. (2009b), Solar energetic-particle release times in historic ground-level events, *Astrophys. J.*, *706*(1), 844–850.

Rees, M. (1963), Auroral ionization and excitation by incident energetic electrons, *Planet. Space Sci.*, *11*(10), 1209–1218.

Reeves, G., K. McAdams, R. Friedel, and T. O'Brien (2003), Acceleration and loss of relativistic electrons during geomagnetic storms, *Geophys. Res. Lett.*, *30*, 1529, doi:10.1029/2002GL016513.

Rodger, C., M. Clilverd, N. Thomson, R. Gamble, A. Seppälä, E. Turunen, N. Meredith, M. Parrot, J.-A. Sauvaud, and J.-J. Berthelier (2007), Radiation belt electron precipitation into the atmosphere: Recovery from a geomagnetic storm, *J. Geophys. Res.*, *112*, A11307, doi:10.1029/2007JA012383.

Rozanov, E., L. Callis, M. Schlesinger, F. Yang, N. Andronova, and V. Zubov (2005), Atmospheric response to NO_y source due to energetic electron precipitation, *Geophys. Res. Lett.*, *32*, L14811, doi:10.1029/2005GL023041.

Rozanov, E., M. Calisto, T. Egorova, T. Peter, and W. Schmutz (2012), Influence of the precipitating energetic particles on atmospheric chemistry and climate, *Surv. Geophys.*, *33*(3-4), 483–501.

Schröter, J., B. Heber, F. Steinhilber, and M. Kallenrode (2006), Energetic particles in the atmosphere: A Monte Carlo simulation, *Adv. Space Res.*, *37*(8), 1597–1601.

Sinnhuber, M., H. Nieder, and N. Wieters (2012), Energetic particle precipitation and the chemistry of the mesosphere/lower thermosphere, *Surv. Geophys.*, *33*(6), 1281–1334.

Solomon, S. (1993), Auroral electron transport using the Monte Carlo method, *Geophys. Res. Lett.*, *20*(3), 185–188.

Sternheimer, R., M. Berger, and S. Seltzer (1984), Density effect for the ionization loss of charged particles in various substances, *At. Data Nucl. Data Tables*, *30*(2), 261–271.

Stozhkov, Y., N. Svirzhevsky, G. Bazilevskaya, A. Kvashnin, V. Makhmutov, and A. Svirzhevskaya (2009), Long-term (50 years) measurements of cosmic ray fluxes in the atmosphere, *Adv. Space Res.*, *44*(10), 1124–1137.

Tsurutani, B., G. Lakhina, and O. Verkhoglyadova (2013), Energetic electron (> 10 keV) microburst precipitation, ∼5-15s X-ray pulsations, chorus, and wave-particle interactions: A review, *J. Geophys. Res. Space Physics*, *118*, 2296–2312, doi:10.1002/jgra.50264.

Turunen, E., P. Verronen, A. Seppälä, C. Rodger, M. Clilverd, J. Tamminen, C.-F. Enell, and T. Ulich (2009), Impact of different energies of precipitating particles on NO_x generation in the middle and upper atmosphere during geomagnetic storms, *J. Atmos. Sol. Terr. Phys.*, *71*(10–11), 1176–1189.

Usanova, M., et al. (2014), Effect of EMIC waves on relativistic and ultrarelativistic electron populations: Ground-based and Van Allen Probes observations, *Geophys. Res. Lett.*, *41*, 1375–1381, doi:10.1002/2013GL059024.

Usoskin, I., and G. Kovaltsov (2006), Cosmic ray induced ionization in the atmosphere: Full modeling and practical applications, *J. Geophys. Res.*, *111*, D21206, doi:10.1029/2006JD007150.

Usoskin, I. G., L. Desorgher, P. Velinov, M. Storini, E. Flückiger, R. Bütikofer, and G. Kovaltsov (2009), Ionization of the Earth's atmosphere by solar and galactic cosmic rays, *Acta Geophys.*, *57*(1), 88–101.

Usoskin, I. G., G. Kovaltsov, I. Mironova, A. Tylka, and W. Dietrich (2011), Ionization effect of solar particle GLE events in low and middle atmosphere, *Atmos. Chem. Phys.*, *11*, 1979–1988.

Vainio, R., et al. (2009), Dynamics of the Earth's particle radiation environment, *Space Sci. Rev.*, *147*(3–4), 187–231.

Velinov, P., S. Asenovski, K. Kudela, J. Lastovička, L. Mateev, A. Mishev, and P. Tonev (2013), Impact of cosmic rays and solar energetic particles on the Earth's ionosphere and atmosphere, *J. Space Weather Space Clim.*, *3*, A14, doi:10.1051/swsc/2013036.

Verronen, P., C. Rodger, M. Clilverd, and S. Wang (2011), First evidence of mesospheric hydroxyl response to electron precipitation from the radiation belts, *J. Geophys. Res.*, *116*, D07307, doi:10.1029/2010JD014965.

Vitt, F., and C. Jackman (1996), A comparison of sources of odd nitrogen production from 1974 through 1993 in the Earth's middle atmosphere as calculated using a two-dimensional model, *J. Geophys. Res.*, *101*(D3), 6729–6739.

Wissing, J., and M.-B. Kallenrode (2009), Atmospheric ionization module Osnabrück (AIMOS): A 3-D model to determine atmospheric ionization by energetic charged particles from different populations, *J. Geophys. Res.*, *114*(6), A06104, doi:10.1029/2008JA013884.